Coatings **2015**, *5*, 39-53; doi:10.3390/coatings5010039

OPEN ACCESS

coatings

ISSN 2079-6412

www.mdpi.com/journal/coatings

Article

Halogen-Free Phosphonate Ionic Liquids as Precursors of Abrasion Resistant Surface Layers on AZ31B Magnesium Alloy

Tulia Espinosa, José Sanes and María-Dolores Bermúdez *

Grupo de Ciencia de Materiales e Ingeniería Metalúrgica, Departamento de Ingeniería de Materiales y Fabricación, Universidad Politécnica de Cartagena, 30202 Cartagena, Spain;
E-Mails: tulia.espinosa@upct.es (T.E.); pepe.sanes@upct.es (J.S.)

* Author to whom correspondence should be addressed; E-Mail: mdolores.bermudez@upct.es; Tel.: +34-968-325958; Fax: +34-968-326445.

Academic Editor: Alessandro Lavacchi

Received: 5 December 2014 / Accepted: 22 January 2015 / Published: 28 January 2015

Abstract: Surface coatings formed by immersion in the ionic liquids (ILs) 1,3-dimethylimidazolium methylphosphonate (LMP101), 1-ethyl-3-methylimidazolium methylphosphonate (LMP102) and 1-ethyl-3-methylimidazolium ethylphosphonate (LEP102) on magnesium alloy AZ31B at 50 °C have been studied. The purpose of increasing the temperature was to reduce the immersion time, from 14 days at room temperature, to 48 hours at 50 °C. The abrasion resistance of the coated alloy was studied by microscratching under progressively increasing load, and compared with that of the uncoated material. The order of abrasion resistance as a function of the IL is LEP102 > LMP101 > LMP102, which is in agreement with the order obtained for the coatings grown at room temperature. The maximum reduction in penetration depth with respect to the uncovered alloy, of a 44.5%, is obtained for the sample treated with the ethylphosphonate LEP102. However, this reduction is lower than that obtained when the coating is grown at room temperature. This is attributed to the increased thickness and lower adhesion of the coatings obtained at 50 °C, particularly those obtained from methylphosphonate ionic liquids. The results are discussed from SEM-EDX and profilometry.

Keywords: magnesium; ionic liquids; alkylphosphonate; coatings; abrasion

---

1. Introduction

In order to protect the light and highly reactive magnesium alloys from surface damage failures due to corrosion and/or wear, it is necessary to apply surface protecting coatings which prevent or reduce corrosive attack and severe wear [1,2]. Room temperature ionic liquids are fluids composed of ions which are stable in the liquid state at room temperature. They present a variety of properties such as high thermal stability, a wide electrochemical window, high conductivity, negligible volatility and nonflammability, which make them useful in a variety of applications, from solvents to thermal fluids. From the materials science and surface engineering point of view, ionic liquids have shown outstanding potential as lubricants and lubricant additives [3–27] including lubrication of light alloys [14,24,28–34], nanophase modifiers [35,36], electrolytes [37], corrosion inhibitors [38–49] or reagents in the formation of corrosion protective surface coatings [50–52].

Phosphorus-containing coatings, in particular phosphonate derivatives [1,53,54] are currently been studied as corrosion protective layers on magnesium alloys due to their biocompatibility. Phosphorus-containing ionic liquids have been extensively applied in corrosion protection of magnesium alloys [55–64]. Together with corrosion, another major cause of surface failure of magnesium alloys is their poor tribological performance. Even the best lubricants, including ionic liquids fail to reduce friction and protect magnesium against severe wear in sliding against other materials.

Phosphonate imidazolium ionic liquids have shown to be highly reactive towards copper [65]. In a previous work [66], we have shown that AZ31B magnesium alloy can be protected against abrasion by surface layers grown by long-term immersion in phosphonate imidazolium ionic liquids at room temperature. In order to reduce immersion time, we have now studied the effect of temperature on the nature and abrasion resistance of the coatings.

2. Experimental Section

Ionic liquids 1,3-dimethylimidazolium methylphosphonate (LMP101), 1-ethyl-3-methylimidazolium methylphosphonate (LMP102) and 1-ethyl-3-methylimidazolium ethylphosphonate (LEP102) (purity > 98%) (Figure 1) were purchased from Solvionic (Toulouse, France) and used as received.

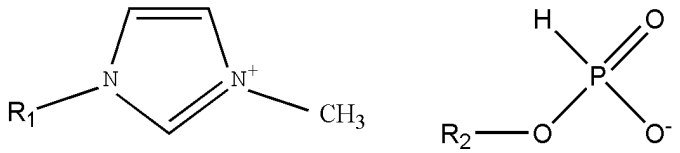

Figure 1. Chemical structure of phosphonate ionic liquids. For LMP101: [$R_1 = R_2 = CH_3–$; For LMP102: $R_1 = CH_3–CH_2–$, $R_2 = CH_3–$; For LEP102: $R_1 = CH_3–CH_2–$, $R_2 = CH_3–CH_2–$.

Magnesium alloy AZ31B (3 wt.% Al; 1 wt.% Zn; 0.6 wt.% Mn; 0.1 wt.% Si; Mg, balance; hardness, 57 HV) test coupons (10 mm × 10 mm × 1.5 mm) were used. The surface was polished to a mean surface roughness (R_a) of 0.22 μm. After covering the surface with the corresponding ionic liquid (1.5 mL approximately), they were heated in an oven at 50 °C during 48 h. After this period of time, no IL remained on the surface which appeared dry and completely covered by the coating layer.

Abrasión tests (Figure 2) were performed using a MTR3/50-50/NI (Microtest, Madrid, Spain) microscratching equipment. Friction coefficients and penetration depths (P_d) were determined along a 3 mm distance, under a progressively increasing normal load between 0 and 30 N, applied by a diamond indenter (200 μm diameter; 120° cone angle), using an inductive probe with a measuring range of ±250 μm and a precision of ±0.5 μm, as previously described [35].

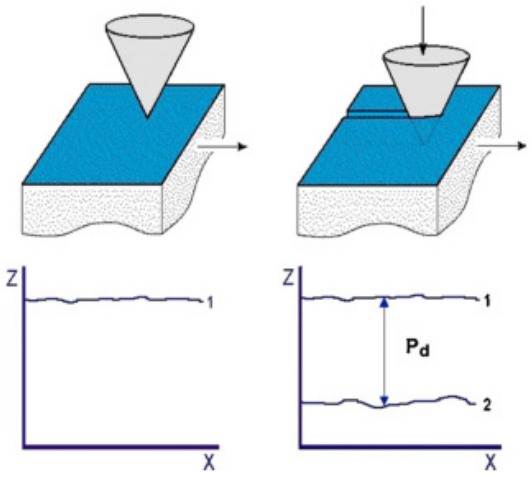

Figure 2. Scheme of the abrasion test configuration (P_d = penetration depth).

SEM/EDX analyses were obtained with a Hitachi S3500 N electron microscope (Hitachi, Tokyo, Japan). Surface roughness values were determined with a Talysurf CLI 500 (Taylor Hobson Ltd., Leicester, UK) optical profiler.

3. Results and Discussion

3.1. Growth of Coatings on Mg AZ31B.

Figures 3 and 4 show SEM micrographs, EDX spectra and element maps of the surface layers on AZ31B after treatment with LMP101 and LMP102, respectively.

The EDX spectrum in Figure 3c shows the presence of oxygen, phosphorus and magnesium. Magnesium and phosphorus element maps (Figure 3d) are in agreement with the phosphonate coating grains and the magnesium alloy substrate at the grain boundaries. Similar microstructures have been observed for LMP102. The main differences between the new coatings obtained at 50 °C with respect to those at room temperature [66], apart from the expected increase of reaction velocity, with a reduction in reaction time from 2 weeks to 48 hours, are their larger thickness and poorer adherence, as shown by the lack of coating layer in some regions of the surface (Figure 3a).

In the case of LMP102 (Figure 4a–d), the poor adherence of the coating layer and the starting delamination process of the coating scales can be clearly observed (Figure 4b). As the cracking of the coating layers could be due to the vacuum conditions of the SEM observation, surface topography profiles were observed, to find a discontinuous layer also under ambient conditions (Figure 5). The regions colored in red in Figure 5 correspond to magnesium substrate, clearly visible on the edges of the wear path, but also outside it.

The thickness of the coating obtained from LEP102 (Figure 6) is lower, as can be observed by the lower intensity P and O peaks with respect to that of Mg, as compared with the coatings obtained from the methylphosphonate ionic liquids LMP101 and LMP102 (Figure 4c). This thinner layer can be also observed in the EDX element maps, where the presence of phosphorus is not detected in some regions of the coated surface.

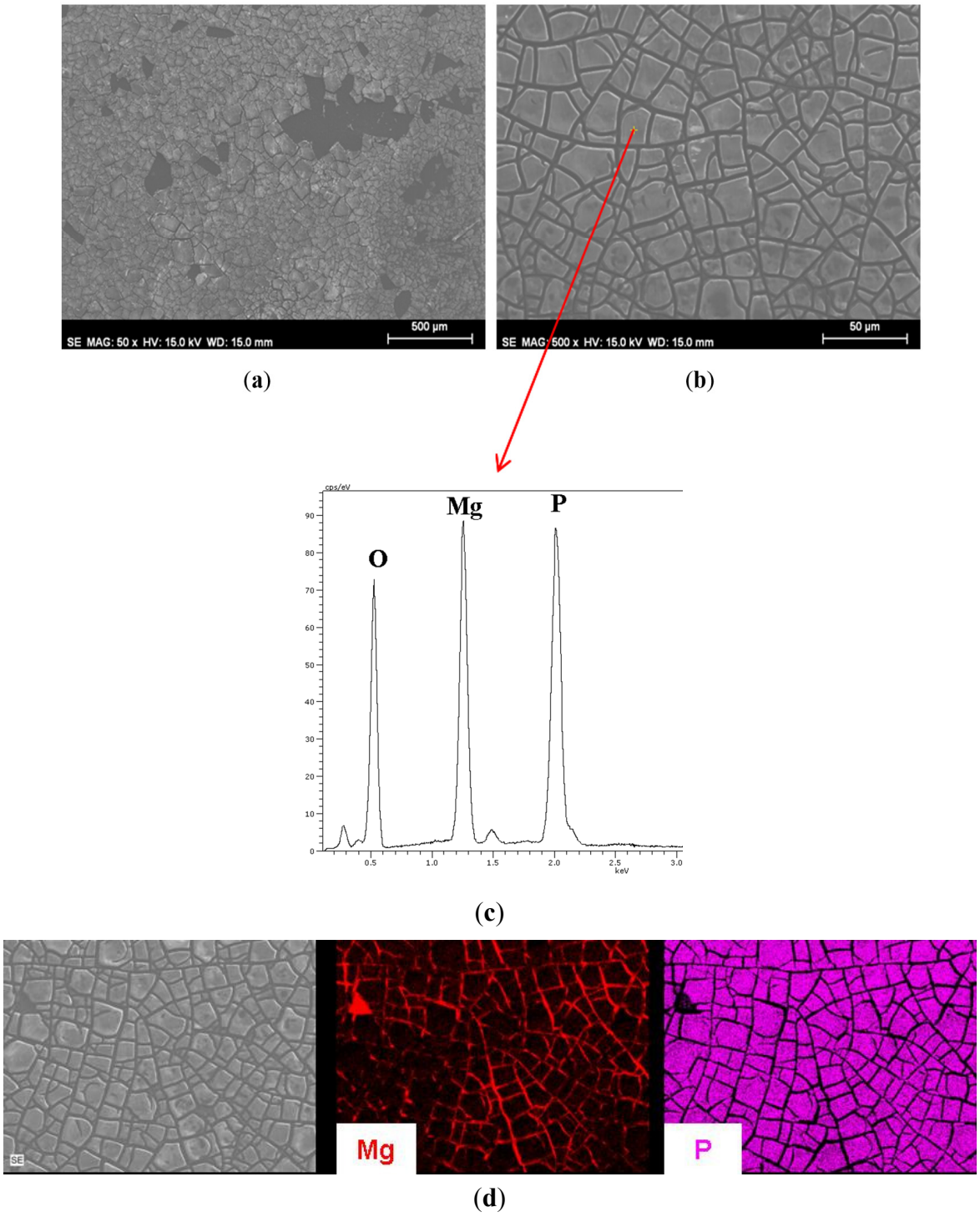

Figure 3. Surface layer on AZ31B after treatment with LMP101: (**a**) SEM micrograph; (**b**) Magnification; (**c**) EDX spectrum; (**d**) Magnesium and phosphorus element maps.

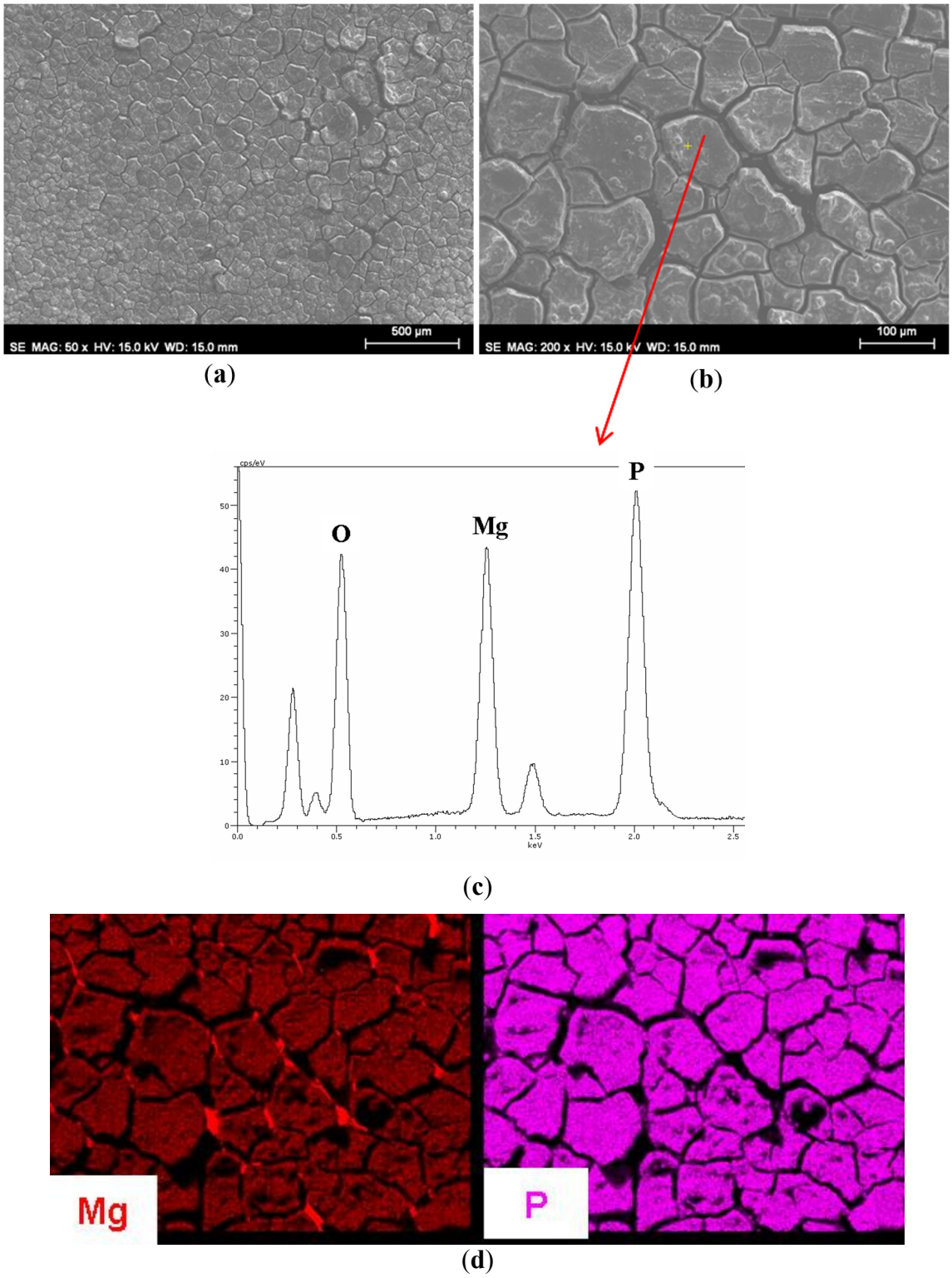

Figure 4. Surface layer on AZ31B after treatment with LMP102: (**a**) SEM micrograph; (**b**) Magnification; (**c**) EDX spectrum; (**d**) Magnesium and phosphorus element maps.

The observed differences in the coating layers obtained from the ethylphosphonate ionic liquid LEP102 and the methylphosphonate ionic liquids LMP101 and LMP102 could be related to a lower reactivity due to the longer alkyl chain on the phosphonate anion of LEP102.

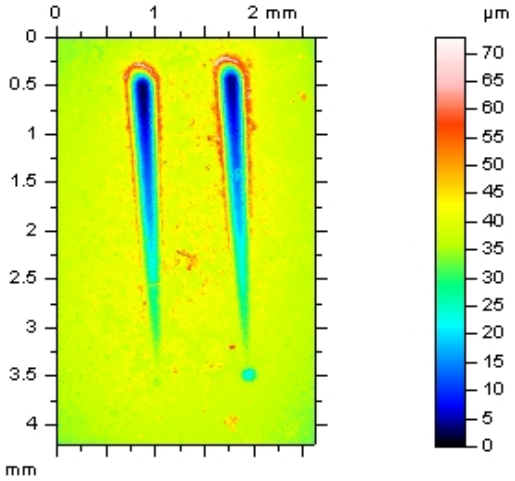

Figure 5. Surface topography profiles of wear scars on AZ31B after treatment with LMP102.

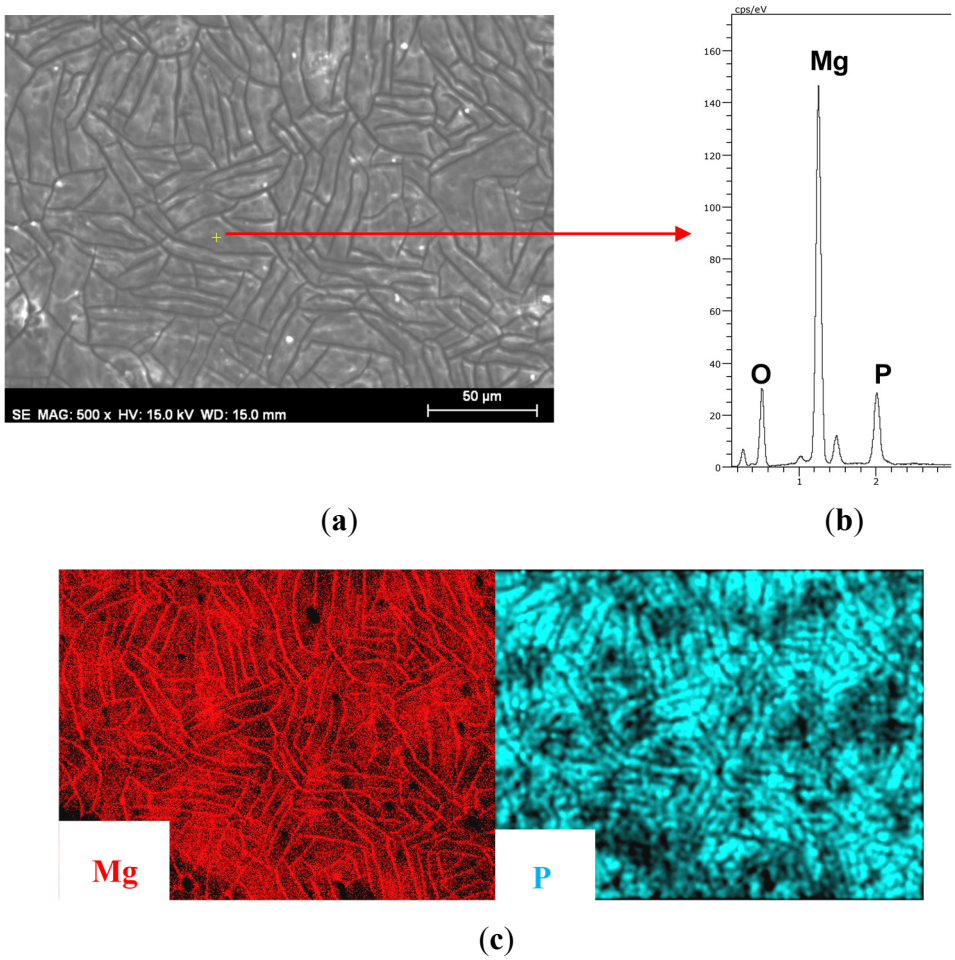

Figure 6. Surface layer on AZ31B after treatment with LEP102: (**a**) SEM micrograph; (**b**) EDX spectrum; (**c**) Magnesium and phosphorus element maps.

The presence of intermetallic aluminum-rich precipitates in the microstructure of AZ31B can be observed in Figure 6a as white rounded precipitates and, more clearly, in the EDX element map in Figure 7.

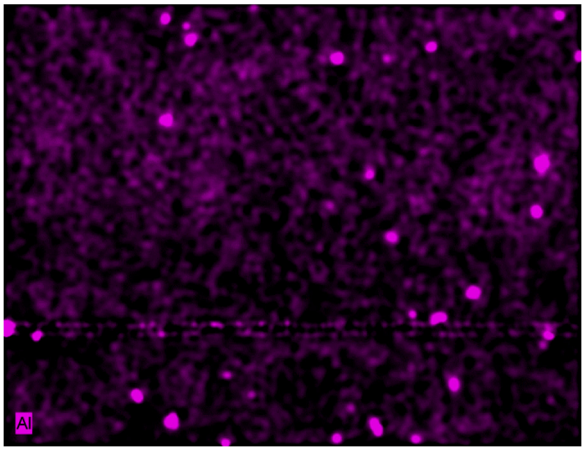

Figure 7. Al element map of AZ31B after treatment with LEP102.

The higher adherence and lower thickness of the more continuous coating obtained form LEP102, gives rise to a lower roughness increase with respect to the base alloy than that observed for the rest of ionic liquids (Table 1).

Table 1. Surface roughness.

Material	R_a (μm) (standard deviation)
AZ31B	0.22 (0.03)
AZ31B + LEP102	0.34 (0.03)
AZ31B + LMP101	0.68 (0.08)
AZ31B + LMP102	2.10 (0.31)

3.2. Abrasion Resistance of the New Coatings

Figure 8 shows the variation of the friction coefficients with increasing normal load under scratching for the four materials, the uncoated AZ31B alloy and the AZ31B coated with the layers obtained from each of the ionic liquids. There is a good agreement between roughness values (Table 1) and friction coefficients, with a lower resistance to sliding for the more polished surfaces.

The lowest friction coefficient is obtained for the uncoated alloy, with the most polished surface, while the highest friction coefficient is obtained for the material with the highest average roughness, covered with the layer generated from LMP102.

Figure 9 compares the evolution of penetration depth values with increasing normal load for the uncoated alloy and the alloy covered with the surface layers from the three ionic liquids. AZ31B alloy shows an approximately linear increase in penetration depth up to 10N. At that point, a transition to more severe abrasion wear takes place, as observed by the slope increase in the penetration depth curve. Finally, for loads higher than 20 N, an asymptote is reached. Under low loads, up to 10 N, the layer generated from LMP101 shows the lowest abrasion resistance, while the behavior of the layer from LMP102 is similar to that of the uncoated alloy.

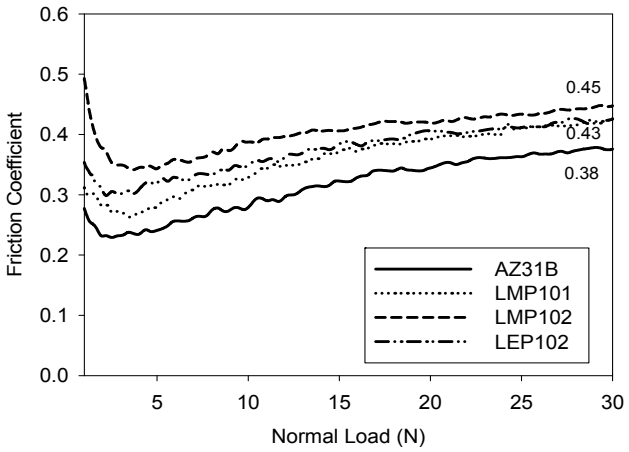

Figure 8. Friction coefficients as a function of the applied normal load.

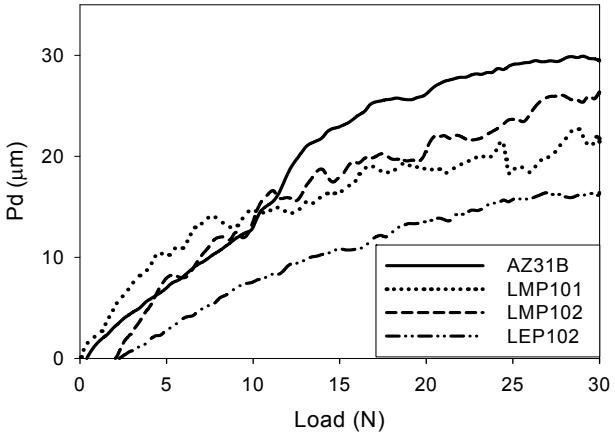

Figure 9. Penetration depths (Pd) as a function of normal load.

For normal loads higher than 10 N, all coatings show a better abrasion resistance than the base alloy, in the order: LEP102 > LMP101 > LMP102 > AZ31B. Under the maximum load of 30 N the penetration depth reductions with respect to AZ31B are of a 27.6% for LMP101, a 11.5% for LMP102 and a 44.5% for LEP102. It is important to notice that only the layer from LEP102 improves abrasion resistance of AZ31B under the whole range of applied loads.

Figure 10a–e shows SEM micrographs of one of the wear tracks on the material covered with the layer formed with LMP102. Figure 10a shows the severe surface damage at the tip of the wear track, under the highest normal applied load of 30 N. The coating has been eliminated, not only along the wear path, but also on extensive areas outside the wear track.

Figure 10b shows the presence of wear debris particles from the surface coating. These are large platelets with a mean thickness of 6–7 μm. Figure 10c,d shows the increasing severity of the fracture and removal of the coating as normal load increases. This mechanism explains the high friction coefficient values (Figure 8). Finally, Figure 10e shows the fracture under the initial application of load at the start of the wear path, with the corresponding decreases of the size of coating grains. A similar wear mechanism is observed in the case of LMP101. These observations are in contrast with the thinner layer obtained from LEP102. A possible explanation for this could be the higher reactivity of the ionic liquids with shorter alkyl substituents.

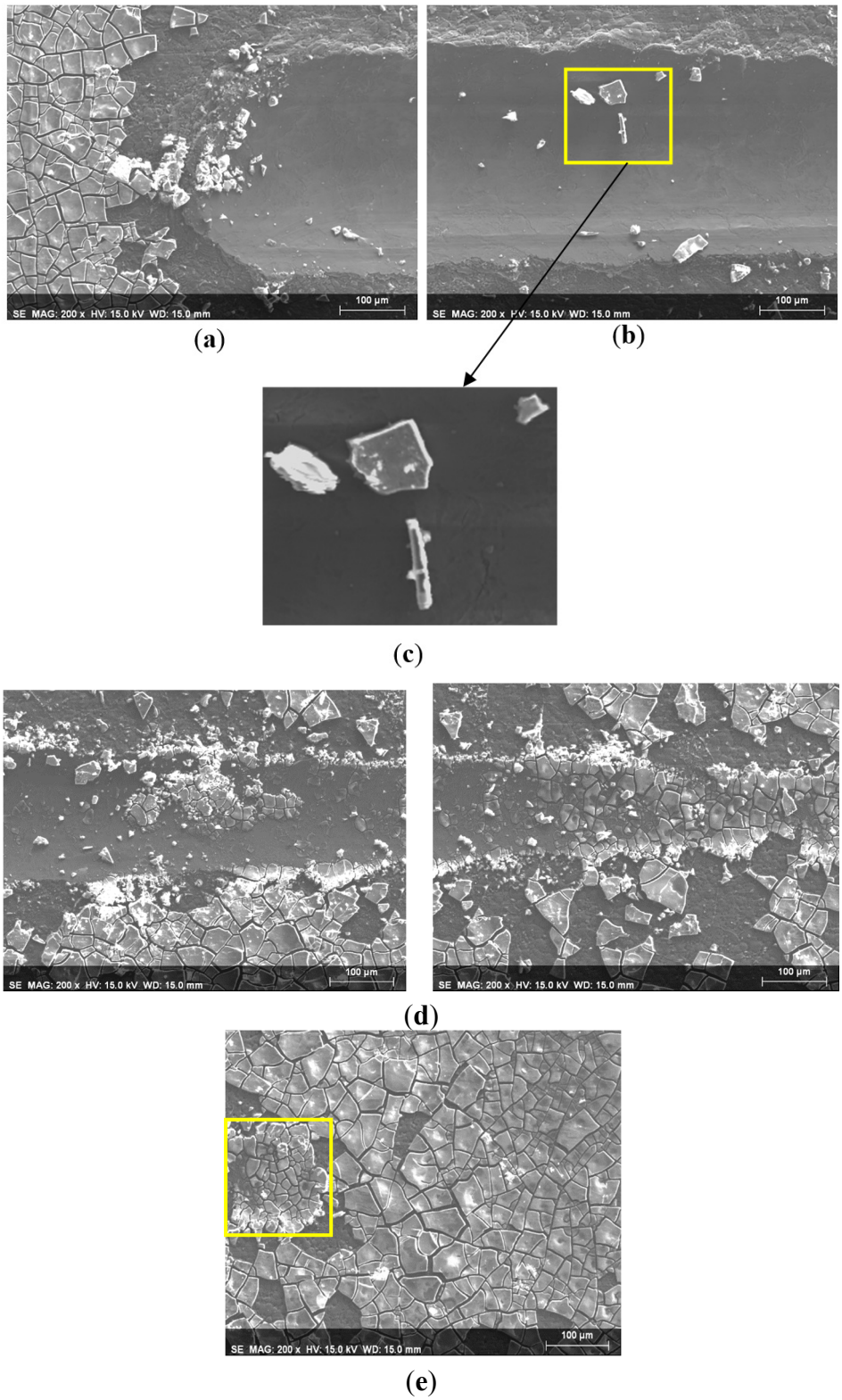

Figure 10. SEM micrographs of the wear path on AZ31B with layer from LPM102: (**a**) Wear track under 30 N; (**b**) Wear track under 2–25 N, with magnified detail of wear debris; (**c**–**d**) Wear track under 5–20 N; (**e**) Wear track under 0–5 N, with detail of the area where load application starts.

Figure 11a–c show SEM micrographs of the different regions of the wear track on the coating obtained from LEP102, from lower load (Figure 11a) to maximum applied load (Figure 11c). In this case, no fracture or generation of wear debris particles form the coating layer is observed. A smother wear track surface is obtained, where the surface layer penetrates into the magnesium alloy substrate due to the applied load.

The phosphorus and magnesium element maps in Figure 12 show that, up to 10 N, the whole or large areas of the wear track remain covered by the phosphorus containing layer. From that load on, although large areas of magnesium from the substrate are present at the surface, coating particles remain within the wear track, even under the highest applied load at the end of the track. This mechanism is similar to that observed for the coating obtained at room temperature [66] and is in sharp contrast with the coating failure observed for the methylphosphonates LMP101 and LMP102 (Figure 9). This could be attributed to the better adherence of the thinner layer generated from the ethylphosphonate LEP102.

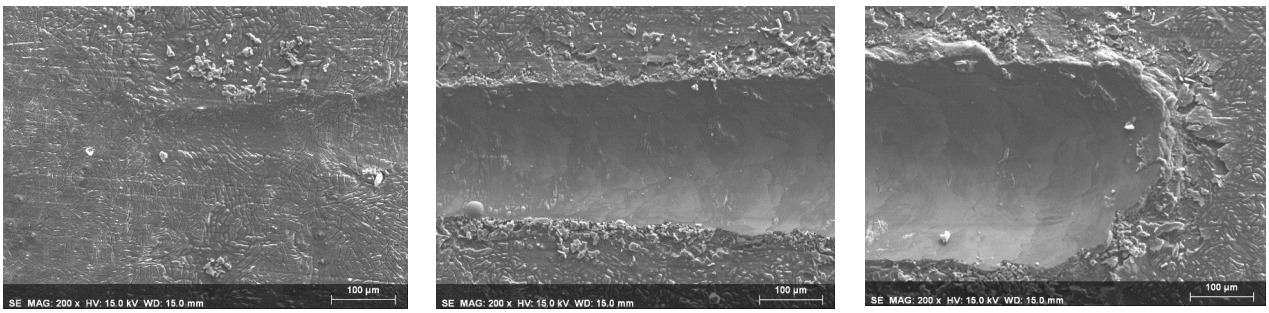

(**a**) (**b**) (**c**)

Figure 11. SEM micrographs along the wear track on AZ31B coated with the layer generated from LEP102: (**a**) Low load; (**b**) Intermediate load; (**c**) Maximum load.

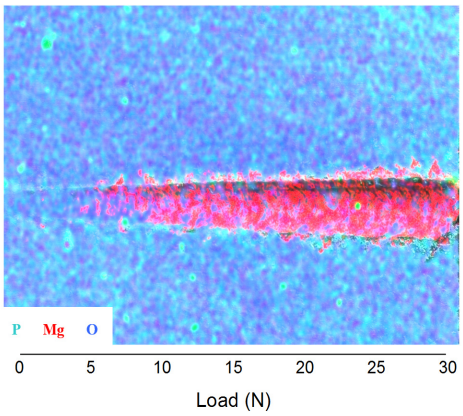

Figure 12. EDX element map of the wear track on AZ31B coated with the layer generated from LEP102 along the whole range of applied loads.

4. Conclusions

Alkylphosphonate ionic liquids react with the AZ31B magnesium alloy to form phosphorus-containing surface layers able to reduce the surface damage due to abrasion. At 50 °C, the reaction time is reduced from 14 days, at room temperature, to 48 hours.

The new coatings present higher friction coefficients due to the increase in surface roughness with respect to the base alloy. The highest surface roughness is obtained for the coatings generated from methylphosphonate ionic liquids.

In the case of the methylphosphonate ionic liquids, the coating layers obtained at 50 °C are 6–7 μm thick and present a very poor adherence to the substrate alloy. This is the main cause for the delamination and failure of the coating under abrasion. In this way, the surface layers obtained from methylphosphonate ionic liquids only reduce the penetration depth under loads higher than 10 N, after the base alloy has experienced a transition to more severe wear.

In contrast, the ethylphosphonate ionic liquid is less reactive, giving rise to a very thin coating, with a lower proportion of phosphorus, which shows a better adherence and absence of delamination under load. This thinner coating shows the highest abrasion resistance and reduces penetration depth in a 44.5% with respect to the uncoated alloy.

In order to reduce reaction times, electrochemical processes are currently being studied to develop protective surface coatings from phosphonate ionic liquids.

Acknowledgments

The authors wish to thank the financial support of the Ministerio de Economía y Competitividad (MINECO, Spain), grants: MAT2011-23162 and MAT2014-55384-P. T. Espinosa is grateful to Ministerio de Educación, Cultura y Deporte (MECD, Spain) for a research FPU grant (AP2010-3485).

Author Contributions

T.E. performed the experiments under the supervision of J.S. and M.D.B. All authors contributed equally to the design of the experiments and analysis of the data. M.D.B. wrote the paper with the cooperation of J.S. and T.E.

Conflicts of Interest

The authors declare no conflict of interest.

References

1. Khramov, A.N.; Balbyshev, V.N.; Kasten, L.S.; Mantz, R.A. Sol-gel coatings with phosphonate functionalities for surface modification of magnesium alloys. *Thin Solid Films* **2006**, *514*, 174–181.
2. Taltavull, C.; Lopez, A.J.; Torres, B.; Rams, J. Dry sliding wear behaviour of laser surface melting treated AM60B magnesium alloy. *Surf. Coat. Technol.* **2013**, *236*, 368–379.
3. Minami, I. Ionic liquids in tribology. *Molecules* **2009**, *14*, 2286–2305.
4. Zhou, F.; Liang, Y.; Liu, W. Ionic liquid lubricants: Designed chemistry for engineering applications. *Chem. Soc. Rev.* **2009**, *38*, 2590–2599.
5. Bermúdez, M.D.; Jiménez, A.E.; Sanes, J.; Carrion, F.J. Ionic liquids as advanced lubricant fluids. *Molecules* **2009**, *14*, 2888–2908.
6. Torimoto, T.; Tsuda, T.; Okazaki, K.; Kuwabata, S. New frontiers in materials science opened by ionic liquids. *Adv. Mater*. **2010**, *22*, 1196–1221.

7. Palacio, M.; Bhushan, B. A review of ionic liquids for green molecular lubrication in nanotechnology. *Tribol. Lett.* **2010**, *40*, 247–268.
8. Schluecker, E.; Wasserscheid, P. Ionic liquids in mechanical engineering. *Chem. Ing. Tech.* **2011**, *83*, 1476–1484.
9. Somers, A.; Howlett, P.; MacFarlane, D.R.; Forsyth, M. A review of ionic liquid lubricants. *Lubricants* **2013**, *1*, 3–21.
10. Angell, C.A.; Ansari, Y.; Zhao, Z.F. Ionic liquids: Past, present and future. *Faraday Discuss* **2012**, *154*, 9–27.
11. Bermúdez, M.D. Introduction to the ionic liquids special issue. *Tribol. Lett.* **2010**, *40*, 213.
12. Cai, M.; Zhao, Z.; Liang, Y.; Zhou, F. Alkyl imidazolium ionic liquids as friction reduction and anti-wear additive in polyurea grease for steel/steel contacts. *Tribol. Lett.* **2010**, *40*, 215–224.
13. Minami, I.; Inada, T.; Sasaki, R.; Nanao, H. Tribo-chemistry of phosphonium-derived ionic liquids. *Tribol. Lett.* **2010**, *40*, 225–235.
14. Jiménez, A.E.; Bermúdez, M.D. Ionic liquids as lubricants of titanium–steel contact. Part 3. Ti6Al4V lubricated with imidazolium ionic liquids with different alkyl chain lengths. *Tribol. Lett.* **2010**, *40*, 237–246.
15. González, R.; Hernández-Battez, A.; Blanco, D.; Viesca, J.L.; Fernández-González, A. Lubrication of TiN, CrN and DLC PVD coatings with 1-butyl-1-methylpyrrolidinium tris(pentafluoroethyl)trifluorophosphate. *Tribol. Lett.* **2010**, *40*, 269–277.
16. Somers, A.E.; Howlett, P.C.; Sun, J.; MacFarlane, D.R.; Forsyth, M. Transition in wear performance for ionic liquid lubricants under increasing load. *Tribol. Lett.* **2010**, *40*, 279–284.
17. Dörr, N. Special issue on ionic liquids as lubricants. *Proc. Ins. Mech. Eng. Part J J. Eng. Tribol.* **2012**, *226*, 889–890.
18. Minami, I.; Inada, T.; Okada, Y. Tribological properties of halogen-free ionic liquids. *Proc. Ins. Mech. Eng. Part J J. Eng. Tribol.* **2012**, *226*, 891–902.
19. Lucia Pisarova, L.; Steudte, S.; Dörr, N.; Pittenauer, E.; Allmaier, G.; Stepnowski, P.; Stolte, S. Ionic liquid long-term stability assessment and its contribution to toxicity and biodegradation study of untreated and altered ionic liquids. *Proc. Ins. Mech. Eng. Part J J. Eng. Tribol.* **2012**, *226*, 903–922.
20. Pejaković, V.; Kronberger, M.; Mahrova, M.; Vilas, M.; Tojo, E.; Kalin, M. Pyrrolidinium sulfate and ammonium sulfate ionic liquids as lubricant additives for steel/steel contact lubrication. *Proc. Ins. Mech. Eng. Part J J. Eng. Tribol.* **2012**, *226*, 923–932.
21. Kronberger, M.; Pejaković, V.; Gabler, C.; Kalin, M. How anion and cation species influence the tribology of a green lubricant based on ionic liquids. *Proc. Ins. Mech. Eng. Part J J. Eng. Tribol.* **2012**, *226*, 933–951.
22. Pagano, F.; Gabler, C.; Zare, P.; Mahrova, M.; Dörr, N.; Bayon, R.; Fernandez, X.; Binder, W.H.; Hernaiz, M.; Tojo, E.; *et al*. Dicationic ionic liquids as lubricants. *Proc. Ins. Mech. Eng. Part J J. Eng. Tribol.* **2012**, *226*, 952–964.
23. Mendonça, A.C.F.; Dörr, N.; Pádua, A.A.H. Predicting thermophysical properties of ionic liquids as a function of temperature and pressure. *Proc. Ins. Mech. Eng. Part J J. Eng. Tribol.* **2012**, *226*, 965–976.

24. Bermúdez, M.D.; Jiménez, A.E. Surface interactions in lubrication of titanium, aluminium, and titanium–aluminium alloys with the ionic liquid [C_2mim]Tf_2N under increasing temperature. *Proc. Ins. Mech. Eng. Part J J. Eng. Tribol.* **2012**, *226*, 977–990.
25. Kondo, Y.; Yagi, S.; Koyama, T.; Tsuboi, R.; Sasaki, S. Lubricity and corrosiveness of ionic liquids for steel-on-steel sliding contacts. *Proc. Ins. Mech. Eng. Part J J. Eng. Tribol.* **2012**, *226*, 991–1006.
26. Predel, T.; Pohrer, B.; Schluecker, E. Ionic liquids as alternative lubricants for special applications. *Chem. Eng. Technol.* **2010**, *33*, 132–136.
27. Espinosa, T.; Jiménez, M.; Sanes, J.; Jimenez, A.E.; Iglesias, M.; Bermudez, M.D. Ultralow friction with a protic ionic liquid boundary film at the water-lubricated sapphire-stainless steel interface. *Tribol. Lett.* **2014**, *53*, 1–9.
28. Jimenez, A.E.; Bermudez, M.D. Ionic liquids as lubricants of titanium-steel contact. Part 2: Friction, wear and surface interactions at high temperature. *Tribol. Lett.* **2010**, *37*, 431–443.
29. Jimenez, A.E.; Bermudez, M.D. Ionic liquids as lubricants of titanium-steel contact. *Tribol. Lett.* **2009**, *33*, 111–126.
30. Somers, A.E.; Khemchandani, B.; Howlett, P.C.; Sun, J.Z.; MacFarlane, D.R.; Forsyth, M. Ionic liquids as antiwear additives in base oils: Influence of structure on miscibility and antiwear performance for steel on aluminium. *ACS Appl. Mater. Inter.* **2013**, *5*, 11544–11553.
31. Somers, A.E.; Biddulph, S.M.; Howlett, P.C.; Sun, J.Z.; MacFarlane, D.R.; Forsyth, M. A comparison of phosphorus and fluorine containing IL lubricants for steel on aluminum. *Phys. Chem. Chem. Phys.* **2012**, *14*, 8224–8231.
32. Qiao, D.; Wang, H.Z.; Feng, D.P. Tribological performance of phosphate ionic liquids as lubricants for steel-on-aluminum contacts. *Proc. Inst. Mech. Eng. Part J J. Eng. Tribol.* **2013**, *227*, 1261–1271.
33. Jiang, D.; Hu, L.T.; Feng, D.P. Tribological behaviours of novel crown-type phosphate ionic liquids as lubricants for steel/aluminium contacts. *Ind. Lubr. Tribol.* **2013**, *65*, 219–225.
34. Qiao, D.; Wang, H.; Feng, D. Tribological performance and mechanism of phosphate ionic liquids as additives in three base oils for steel-on-aluminum contact. *Tribol. Lett.* **2014**, *55*, 517–531.
35. Espejo, C.; Carrión, F.J.; Bermúdez, M.D. Scratch resistance of new polystyrene nanocomposites with ionic liquid-modified multi-walled carbon nanotubes. *Tribol. Lett.* **2013**, *52*, 271–285.
36. Saurín, N.; Sanes, J.; Bermudez, M.D. Effect of graphene and ionic liquid additives on the tribological performance of epoxy resin. *Tribol. Lett.* **2014**, *56*, 133–142.
37. Zhang, S.J.; Sun, J.; Zhang, X.C.; Xin, J.Y.; Miao, Q.Q.; Wang, J.J. Ionic liquid-based green processes for energy production. *Chem. Soc. Rev.* **2014**, *43*, 7838–7869.
38. Ashassi-Sorkhabi, H.; Es'haghi, M. Corrosion inhibition of mild steel in acidic media by [BMIm]Br ionic liquid. *Mater. Chem. Phys.* **2009**, *114*, 267–271.
39. Zhang, Q.B.; Hua, Y.X. Corrosion inhibition of mild steel by alkylimidazolium ionic liquids in hydrochloric acid. *Electrochim. Acta* **2009**, *54*, 1881–1887.
40. Shukla, S.K.; Murulana, L.C.; Ebenso, E.E. Inhibitive effect of imidazolium based aprotic ionic liquids on mild steel corrosion in hydrochloric acid medium. *Int. J. Electrochem. Sci.* **2011**, *6*, 4286–4295.
41. Ibrahim, M.A.M.; Messali, M.; Moussa, Z.; Alzahrani, A.Y.; Alamry, B.; Hammouti, S.N. Corrosion inhibition of carbon steel by imidazolium and pyridinium cations ionic liquids in acidic environment. *Port. Electrochim. Acta* **2011**, *29*, 375–389.

42. Zarrouk, A.; Messali, M.; Zarrok, H.; Salghi, R.; Ali, A.A.; Hammouti, B.; Al-Deyab, S.S.; Bentiss, F. Synthesis, characterization and comparative study of new functionalized imidazolium-based ionic liquids derivatives towards corrosion of C38 steel in molar hydrochloric acid. *Int. J. Electrochem. Sci.* **2012**, *7*, 6998–7015.
43. Likhanova, N.V.; Domínguez-Aguilar, M.A.; Olivares-Xometl, O.; Nava-Entzana, N.; Arce, E.; Dorantes, H. The effect of ionic liquids with imidazolium and pyridinium cations on the corrosion inhibition of mild steel in acidic environment. *Corros. Sci.* **2010**, *52*, 2088–2097.
44. Guzmán-Lucero, D.; Olivares-Xometl, O.; Martínez-Palou, R.; Likhanova, N.V.; Domínguez-Aguilar, M.A.; Garibay-Febles, V. Synthesis of selected vinylimidazolium ionic liquids and their effectiveness as corrosion inhibitors for carbon steel in aqueous sulfuric acid. *Ind. Eng. Chem. Res.* **2011**, *50*, 7129–7140.
45. Likhanova, N.V.; Olivares-Xometl, O.; Guzmán-Lucero, D.; Domínguez-Aguilar, M.A.; Nava, N.; Corrales-Luna, M.; Mendoza, M.C. Corrosion inhibition of carbon steel in acidic environment by imidazolium ionic liquids containing vinyl-hexafluorophosphate as anion. *Int. J. Electrochem. Sci.* **2011**, *6*, 4514–4536.
46. Tüken, T.; Demir, F.; Kicir, N.; Sigircik, G.; Erbil, M. Inhibition effect of 1-ethyl-3-methylimidazolium dicyanamide against steel corrosion. *Corros. Sci.* **2012**, *59*, 110–118.
47. Barham, H.A.; Brahim, S.A.; Rozita, Y.; Mohamed, K.A. Carbon steel corrosion behaviour in aqueous carbonated solution of MEA/bmim DCA. *Int. J. Electrochem. Sci.* **2011**, *6*, 181–198.
48. Zhou, X.; Yang, H.; Wang, F. [BMIM]BF_4 ionic liquids as effective inhibitor for carbon steel in alkaline chloride solution. *Electrochim. Acta* **2011**, *56*, 4268–4275.
49. Scendo, M.; Uznanska, J. The effect of ionic liquids on the corrosion inhibition of copper in acidic chloride solutions. *Int. J. Corros.* **2011**, *2011*, doi:10.1155/2011/718626.
50. Abbott, A.P.; McKenzie, K.J. Application of ionic liquids to the electrodeposition of metals. *Phys. Chem. Chem. Phys.* **2006**, *8*, 4265–4279.
51. Endres, F.; MacFarlane, D.R.; Abbott, A. *Electrodeposition from Ionic Liquids*; Wiley-VCH Verlag GmbH: Weinheim, Germany, 2008.
52. Abbott, A.P.; Frisch, G.; Ryder, K.S. Electroplating using ionic liquids. *Ann. Rev. Mater. Res.* **2013**, *43*, 335–358.
53. Grubac, Z.; Metikos-Hukovic, M.; Roncevic, I.S.; Petravic, M.; Peter, R. Functionalization of biodegradable magnesium alloy implants with alkylphosphonate self-assembled films. *Mater. Sci. Eng. C Mater. Biol. Appl.* **2013**, *33*, 2152–2158.
54. Hoque, E.; De Rose, J.A.; Hoffmann, P.; Mathieu, H.J.; Bhushan, B.; Cichomski, M. Phosphonate self-assembled monolayers on aluminium surfaces. *J. Chem. Phys.* **2006**, *124*, doi:10.1063/1.2186311.
55. Forsyth, M.; Howlett, P.C.; Tan, S.K.; MacFarlane, D.R.; Birbilis, N. An ionic liquid surface treatment for corrosion protection of magnesium alloy AZ31. *Electrochem. Solid-State Lett.* **2006**, *9*, B52–B55.
56. Birbilis, N.; Howlett, P.C.; MacFarlane, D.R.; Forsyth, M. Exploring corrosion protection of Mg via ionic liquid pretreatment. *Surf. Coat. Technol.* **2007**, *201*, 4496–4504.
57. Howlett, P.C.; Zhang, S.; MacFarlane, D.R.; Forsyth, M. An investigation of a phosphinate-based ionic liquid for corrosion protection of magnesium alloy AZ31. *Aus. J. Chem.* **2007**, *60*, 43–46.

58. Howlett, P.C.; Efthimiadis, J.; Hale, P.; van Riessen, G.A.; MacFarlane, D.R.; Forsyth, M. Characterization of the magnesium alloy AZ31 surface in the ionic liquid trihexyl(tetradecyl)phosphonium bis(trifluoromethanesulfonyl)amide. *J. Electrochem. Soc.* **2010**, *157*, C392–C398.
59. Howlett, P.C.; Khoo, T.; Mooketsi, G.; Efthimiadis, J.; MacFarlane, D.R.; Forsyth, M. The effect of potential bias on the formation of ionic liquid generated surface films on Mg alloys. *Electrochim. Acta* **2010**, *55*, 2377–2383.
60. Sun, J.; Howlett, P.C.; MacFarlane, D.R.; Lin, J.; Forsyth, M. Synthesis and physical property characterisation of phosphonium ionic liquids based on $P(O)_2(OR)_2$- and $P(O)_2(R)_2$-anions with potential application for corrosion mitigation of magnesium alloys. *Electrochim. Acta* **2008**, *54*, 254–260.
61. Efthimiadis, J.; Neil, W.C.; Bunter, A.; Howlett, P.C.; Hinton, B.R.W.; MacFarlane, D.R.; Forsyth, M. Potentiostatic control of ionic liquid surface film formation on ZE41 magnesium alloy. *ACS Appl. Mater. Inter.* **2010**, *2*, 1317–1323.
62. Forsyth, M.; Neil, W.C.; Howlett, P.C.; MacFarlane, D.R.; Hinton, B.R.W.; Rocher, N.; Kemp, T.F.; Smith, M.E. New insights into the fundamental chemical nature of ionic liquid film formation on magnesium alloy surfaces. *ACS Appl. Mater. Inter.* **2009**, *1*, 1045–1052.
63. Huang, P.P.; Latham, J.A.; MacFarlane, D.R.; Howlett, P.C.; Forsyth, M. A review of ionic liquid surface film formation on Mg and its alloys for improved corrosion performance. *Electrochim. Acta* **2013**, *110*, 501–510.
64. Elsentriecy, H.H.; Luo, H.M.; Meyer, H.M.; Grado, L.L.; Qu, J. Effects of pre-treatment and process temperature of a conversion coating produced by an aprotic ammonium-phosphate ionic liquid on magnesium corrosion protection. *Electrochim. Acta* **2014**, *123*, 58–65.
65. Espinosa, T.; Sanes, J.; Jiménez, A.E.; Bermúdez, M.D. Surface interactions, corrosion processes and lubricating performance of protic and aprotic ionic liquids with OFHC copper. *Appl. Surf. Sci.* **2013**, *273*, 578–597.
66. Espinosa, T.; Jiménez, A.E.; Martínez-Nicolás, G.; Sanes, J. Bermúdez, M.D. Abrasion resistance of magnesium alloys with surface films generated from phosphonate imidazolium ionic liquids. *Appl. Surf. Sci.* **2014**, *320*, 267–273.